Journal of Earth Science, *Vol. 27*, *No. 6*, *p. 998–1007*, *December 2016* *ISSN 1674-487X*
Printed in China
DOI: 10.1007/S12583-016-0904-0

Structural Development of Northwest Saudi Arabia Using Aeromagnetic and Seismological Data

Mohamed Fnais[1], **Elkhedr Ibrahim***[1, 2], **Essam Abd El-Motaal**[1, 3], **Kamal Abdelrahman**[1, 4], **Abdelmaguid Al-Heniedi**[1], **Khaled Al-Kahtany**[1]

1. *Department of Geology and Geophysics*, *King Saud University*, *Riyadh* 36002, *KSA*
2. *Department of Geology*, *Faculty of Science*, *Mansoura University*, *Mansoura* 21345, *Egypt*
3. *Department of Geology*, *Faculty of Science*, *Al-Azhar University*, *Cairo* 11435, *Egypt*
4. *Department of Seismology*, *National Research Institute of Astronomy and Geophysics*, *Cairo* 11435, *Egypt*

ABSTRACT: High resolution aeromagnetic and seismological data constrained by field-based structural investigations have been used to map and delineate the structural elements that affected and shaped the Midyan area in the northwest part of Saudi Arabia. The area was divided into four major domains defined by NNE, NNW, NW and ENE trending faults identified by trends, patterns and intensity of magnetic anomalies. The ENE trending left-lateral strike-slip faults intersected by NNE trending faults are the predominant tectonic features in the Gulf of Aqaba coastal area and stop at the boundary of a central domain characterized by complexity in the pattern and intensity of magnetic anomalies, that may be attributed to heterogeneity of basement rocks containing complex igneous rock suites including diorite, gabbro, ultramafic and alkali granitic rocks. This domain is characterized by the presence of narrow linear magnetic anomalies that extend for kilometers in an NNW direction, indicating dikes intruded through NNW trending faults. These dikes become WNW-oriented near their northern termination by transfer of movement to WNW-oriented faults marking the northern termination of the Red Sea rift. It is believed that this fault zone is still experiencing neotectonic activity, as evident from recorded seismicity. The aeromagnetic structural results coincide with fault plane solutions for the largest earthquakes, confirming aeromagnetic interpreted trends and illustrating mixed mechanisms between extensional and strike-slip faulting. Thus the study area displays different mechanisms associated with different tectonic trends which show clearly in the structural patterns of the area.

KEY WORDS: aeromagnetism, seismicity, neotectonics, Midyan area, Saudi Arabia.

0 INTRODUCTION

The study area, the Midyan Peninsula lies in the northwestern most part of the Arabian Plate at the junction of the Red Sea and Gulf of Aqaba. This region has witnessed two most powerful earthquakes that have been experienced in Saudi Arabia during the past three decades and affected inhabited areas of northwestern Saudi Arabia, especially the town of Haql, and occurred in January 1983 and November 1995 (El-Isa et al., 1984). After the latter event, a geological investigation was initiated by the Saudi Geological Survey to identify the youngest fault systems responsible for these earthquakes in Northwest Saudi Arabia and adjacent regions. The understanding of their structural framework was limited by insufficient exposure, which led to difficulty in developing links between local and regional tectonics and resulted in poorly constrained models of the regional-scale structures. High-resolution aeromagnetic data allowed interpretation and modeling at a scale comparable to structural mapping. Therefore, the present study delineates structural elements using aeromagnetic and seismological data alongside structural field investigation, concentrating on faults and dikes related to tectonic events that have affected the study area as a result of the opening of the Red Sea and Gulf of Aqaba Rifts.

1 GEOLOGIC SETTING

The Midyan region contains Proterozoic stratiform and intrusive rocks; Paleozoic sandstones in the east and Mesozoic to Cenozoic sedimentary rocks in the west (Fig. 1). Proterozoic stratiform rocks are represented by six rock units: Hegaf, Silasia, Zaytah, Hinshan, Amlas and Minaweh formations (Clark, 1987, 1985). The Hegaf Formation is composed of a variety of volcanic, volcanoclastic and subordinate epiclastic rocks metamorphosed in the greenschist facies. They are commonly made up of metamorphosed mafic and felsic tuffs, meta-andesite, metabasalt, meta-agglomerate, amphibolite, mafic schist and metamorphosed siltstone (Davies and Grainger, 1985). The Silasia Formation crops out in the southeastern part of the study area

*Corresponding author: eibrahim@ksu.edu.sa

Manuscript received July 10, 2015.
Manuscript accepted November 1, 2015.

and consists of metamorphosed greywacke, siltstone, andesite tuff, and jaspilite, intruded by diabase sills (Harris, 1985). It rests unconformably on underlying metavolcanic rocks of the Hegaf Formation (Johnson and Trent, 1967). The Zaytah Formation is composed of metamorphosed silicic lava and tuff, tuffite and greywacke, and mafic and felsic schist. It is intruded by gabbroic, dioritic and mafic rocks of the Muwaylih Suite and is separated from the Hegaf Formation by large tracts of granitic rocks. The Hinshan Formation is made up mainly of weakly metamorphosed silicic to intermediate volcanic rocks and associated metasediments. The Zaytah Formation is in contact with the Hinshan Formation in the northern part of Midyan region and is younger in age (Rowaihy, 1985; Al-Rehaili, 1982). The Amlas Formation is probably equivalent in age to the Hinshan Formation and made up of clastic sedimentary rocks, mainly conglomerate and breccia, immature sandstone, greywacke, siltstone, shale and minor quartzite (Clark, 1987). The Minaweh Formation is composed of silicic volcanic and pyroclastic rocks interbedded with mainly coarse-grained clastic sedimentary rocks (Bramkamp et al., 1963), dissected by a few thin mafic and felsic dikes and some minor intrusions of pink felsite (Clark, 1987, 1985).

Paleozoic sandstones crop out in the eastern part of Midyan region and form the extensive Hadabet Hisma or Hisma Plateau (Fig. 1). Upper Cretaceous–Eocene pre-Red Sea rift rocks are represented by the Suqah Group that is made up of the Adaffa, Usfan and Matiyah formations of which only the Adaffa Formation is recognized in the eastern reaches of Midyan region and is considered the oldest sedimentary sequence exposed in the Midyan area. The conglomerate contains granite cobbles and pebbles, phosphatic nodules, dinosaur and turtle bones, and petrified wood fragments. The sandstone is a well sorted quartz arenite (Afifi et al., 1993; Milner et al., 1993).

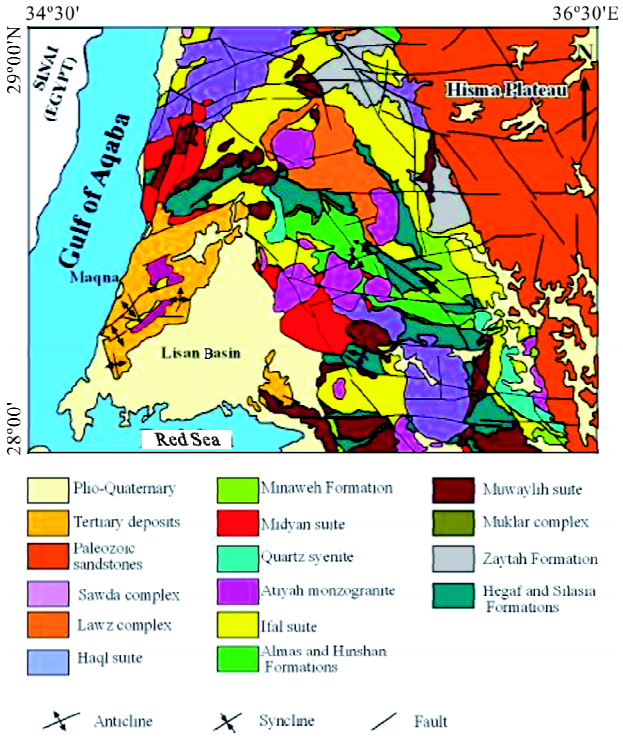

Figure 1. Geologic map of the study area (after Clark, 1987, 1985).

Neogene sedimentary rocks in Midyan area are represented by Tayran Group, Burqan Formation, Maqna Group and Ghawwas and Lisan formations. The Early Miocene Tayran Group comprises Al Wajh, Musayr, and Yanbu formations and is associated with the early period of Red Sea rifting. It is composed of conglomerates, sandstones, shallow-marine carbonates and, at the subsurface, anhydrite (Hughes et al., 1999). The Early to Middle Miocene Maqna Group consists of deep-marine carbonates, shallow-marine carbonates, gypsum and anhydrite, and in the subsurface, deep-marine mudstones and anhydrite. The Late Miocene Ghawwas Formation is a thick succession of interbedded fine and coarse-grained siliciclastics with thin beds of anhydrite. The Lisan Formation is a fluviatile succession that was deposited during the Early Pliocene opening of the Gulf of Aqaba. Five suites of intrusive granitic of regional extent have been recorded in Midyan region (Ramsay et al., 1986). These suites are the Muwaylih, Ifal, Atiya, Haql and Midyan suites. The Midyan Suite represents the last granitic phase of a Pan African thermal event in the evolution of the Arabian Shield (Stoeser, 1986; Radain, 1980) and the Haql granitic suite is intruded by Midyan granite (Al Fotawi et al., 1991).

Block faulting largely controlled the sedimentation and deformation of the study area. The intersections of three major fault systems dominate the area: (1) the Najd system, tending NW-SE, (2) the Red Sea system, trending NNW-SSE and (3) the Gulf of Aqaba system trending NNE-SSW. Most faults in the Midyan region probably date from the Late Proterozoic and were reactivated in the Tertiary. Faults of the Tertiary Red Sea system are present throughout most of the area; fault zones at Jabal az Zuhd and Ash Shiqri are coincident with major negative linear magnetic anomalies (Andreasen and Petty, 1974). Gabbroic dikes of probable Tertiary age (Blank, 1977) are present along fault traces in several places. Mafic dikes also extend away from the lineaments into the country rocks for as much as several kilometers; some of these dikes are Tertiary, but others are older. Motti et al. (1982) revealed that faults having a Red Sea trend were active as far back as the Paleozoic. These faults may have been even older because rocks of the Minaweh Formation in the NNW-trending Aynuna and Sharma troughs (graben), have been protected from erosion since the Late Proterozoic. Faults associated with the Gulf of Aqaba are most obvious within a few kilometers of the coast. Fault movements with both normal and sinistral displacements of several kilometers are evident on individual faults.

3 AEROMAGNETIC DATA PROCESSING

High-resolution aeromagnetic data was acquired in 1982 and 1983 at a terrain clearance of 120 m and line spacing of 2 km, using digital data recording methods. These data are used here as a basis for mapping and delineating subsurface structural elements that affected and shaped the study area. The total magnetic intensity was reduced to the pole (Fig. 2) to overcome bipolarity phenomena. However, reduction to the pole (RTP) of the aeromagnetic data in such low latitudes requires special care to reduce exaggeration of north-south features (Bird, 1997). Declination (41.23º) and inclination (2.6º) determined from IGRF calculations were used for the RTP

transformation. This inconvenience known as amplitude correction can be eliminated by specifying a higher latitude in order to make the amplitude correction alone, but at the expense of under-correcting the amplitudes of north-south features. To achieve the main objective of this study, special filters were used to condition the data set and render the resulting presentation in such a way as to make it easier to interpret the significance of magnetic anomalies in terms of their geological sources (Bird, 1997). The most effective way to filter the data was found to be by using an understanding of the geologic control and the desired filtered results. However, one of the most traditional filters is the separation of long (deep) and short (shallow) wavelength anomalies. The cut-off wavelengths and information about the contribution of such short and long wavelengths in the spectrum could be obtained from the calculated radially-averaged power spectrum of the data. A variety of techniques and filters were applied to remove the shallow magnetic sources and to get better images of the deeper basement structure to produce an upward continuation magnetic anomaly map up to 3 000 m and a regional magnetic anomaly map. To enhance mapping of basaltic flows and near-surface intrusions, an analytic signal (AS) was applied to produce a self-explanatory map that shows the spatial distribution of surface and near-surface volcanic intrusions clearly.

4 AEROMAGNETIC RESULTS

The interpretation of the present aeromagnetic data is constrained by the structural and geological data. A combination of the reduced to the pole (RTP), residual, regional, upward continuation and analytic signal maps should help in investigating the main structural elements and magnetic sources in the study area. The RTP map (Fig. 2) displays magnetic signatures ranging from relatively high intensities (as much as 282 nT) to low magnetic intensities (down to -306 nT). The most obvious feature is the subdivision of the study area into four geologic domains based on magnetic anomaly patterns, trends and intensities. These different domains are separated by major fault systems (Fig. 3). To the east of the study area, an NNW fault separates the broad low magnetic anomaly domain (A) of the Hisma Plateau with its thick cover of Paleozoic sandstone sediments from the middle magnetic domain (B) that is characterized by local rapid variations in the magnetic intensity and anomaly pattern. This fault coincides with edge of the Hisma Plateau and forms a prominent escarpment as much as several hundred meters high in places (Clark, 1985).

The central domain (B) is the Midyan East terrane that contains a complex of igneous rock suites with different rock types ranging from diorite, gabbro and ultramafic rocks to alkali granitic rocks (Davies and Grainger, 1985). Inspection of the magnetic anomalies of domain (B) indicates the presence of linear narrow reversed magnetic anomalies that extend for kilometers in the NNW (Red Sea) trend, as indicated by dashed white lines in Fig. 3. These anomalies are interpreted as dikes intruded through faults that run parallel to the Red Sea structural trend and are probably Early Tertiary in age, associated with the rifting of the Red Sea (Blank, 1977). The coincidence of these dikes along structural weakness zones confirms the conclusion of Motti et al. (1982) and Blank (1977) that these weakness zones originated in the Late or Early Proterozoic and were later rejuvenated in the Tertiary. Similar Tertiary dikes with reversed magnetic anomalies have been recorded in similar structural areas elsewhere in Saudi Arabia (Blank, 1977) and Sinai (Ibrahim et al., 2000). Based on previous geologic literature and field investigations, these dikes are basic dikes which might be expected to show normal magnetic field signatures, so the reversed magnetic signatures of these dikes should be referred to the reversal magnetic field that dominates Tertiary time (Ibrahim et al., 2000).

There is a conspicuous change in direction of these dikes to a WNW-ENE direction when they get close to the Gulf of Aqaba coast (Fig. 3). This can be interpreted as the northern termination of the Red Sea rift where movement has been transferred from NW-oriented faults to pre-existing WNW-

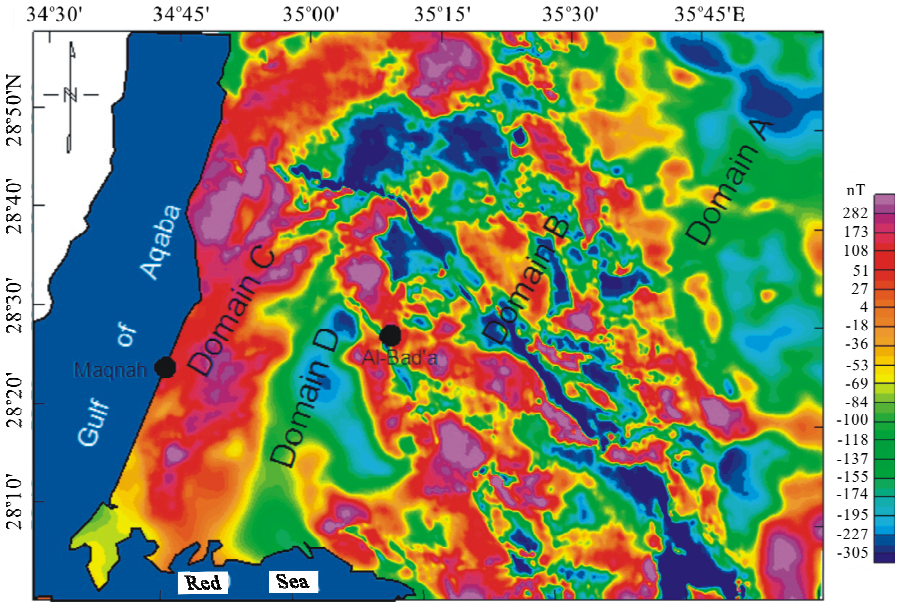

Figure 2. Reduced to the Pole (RTP) magnetic anomaly map with interpreted geologic domains.

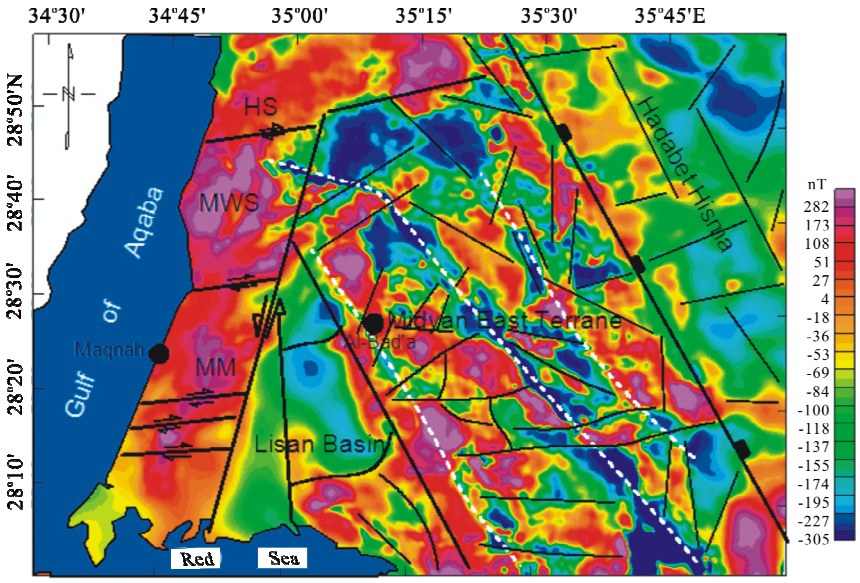

Figure 3. Tectonic interpretation of the RTP magnetic anomaly map. Dashed white lines indicate basic dikes. MM. Maqnah massif; HS. area dominated by the Haql Suite; MWS. area dominated by the Midyan and Muwaylih suites.

oriented faults. The comparable northern termination of the Suez rift, the northern propagation of the Red Sea rift, is suggested by transfer of the throw to other N-W and E-W oriented faults in Cairo-Suez District (Moustafa and Abd-Allah, 1992).

The western domain (C) is characterized by a complex relatively high magnetic anomaly. This complexity could be due to the presence of the Muwaylih Suite that consists of diorite, gabbro and ultramafic rocks (Davies and Grainger, 1985) in contact with the Midyan Suite of alkali granitic rocks and the Haql Suite, a large pluton of pink alkali-feldspar granite towards the north (Fig. 3). These different suites are separated by ENE faults (Remond and Teixido, 1980) that are responsible for bringing these different geologic units in contact. The abrupt change between this domain and the central domain (B) with its complicated magnetic signatures indicates the presence of a fault system that extends in an NNE direction (Fig. 3). Most of the ENE magnetic anomalies are truncated by the Gulf of Aqaba trend (Fig. 3) which strongly suggests that these anomalies have undergone a slight left-lateral offset. This offset of magnetic anomalies confirms the presence of younger motion related to the opening.

There is a wedge-shaped low and broad magnetic anomaly (domain D) appear in the southwest of the study area (Fig. 3) representing depression of the Lisan Basin that formed by the intersection of two NNE and NNW trending faults. This broad low magnetic anomaly is interrupted by a local narrow elongated high magnetic anomaly that could indicate the presence of a Tertiary basaltic dike. This interpreted dike is concealed beneath Pliocene and Pleistocene sands and gravels in the basin. According to KFUPM (1998) such faults have been active since the Middle Miocene and the available seismic data indicates that this fault was active during deposition of the Late Miocene Ghawwas Formation and probably the Pliocene Lisan Formation (Pliocene), indicating that these faults experience neotectonic activity, confirmed by field investigation (Figs. 4a, 4b).

The trends and patterns in the regional magnetic anomaly map (Fig. 5a) and the upward continuation magnetic anomaly map (Fig. 5b) show the presence of the same four main structural domains, which indicates that they formed and were dissected by deep-seated faults. Qualitative interpretation of the two regional maps (Figs. 5a, 5b) reveals the extension of linear magnetic anomalies along NW, NNW, NNE and EW trends indicating that these structural trends have given the study area

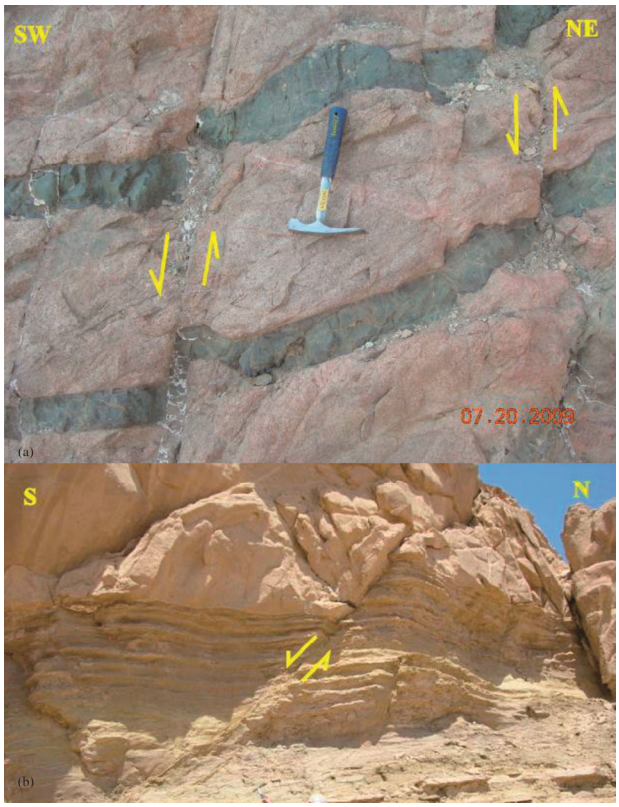

Figure 4. Field photographs showing (a) NE-oriented step faults dissecting an NW-oriented mafic dike hosted by the Muwaylih Suite, and (b) an NNW-oriented listric normal fault dissecting Miocene rocks in the Midyan area.

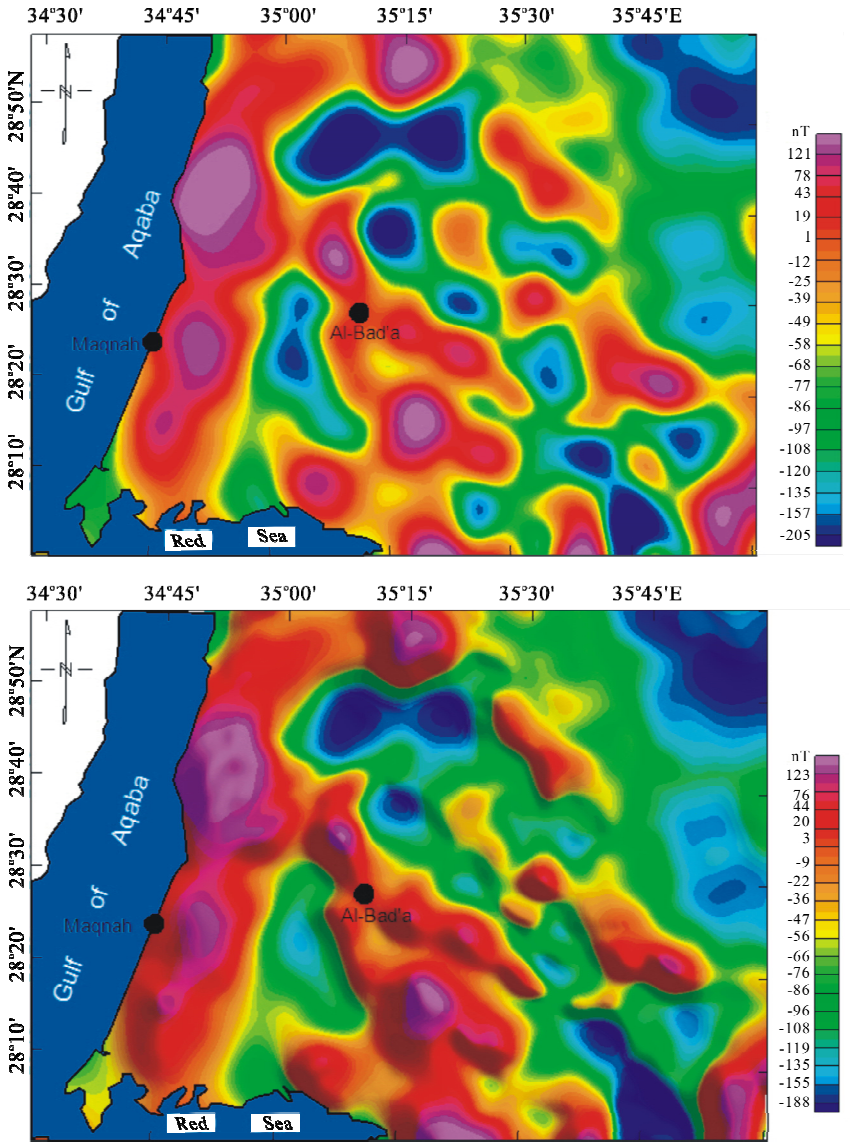

Figure 5. (a) Regional magnetic intensity map and (b) upward continuation to 3 000 m map of the study area.

its triangular configuration due to the intersection of three major fault systems: (1) the Najd system, tending northwest, (2) the Red Sea system, trending north-northwest and (3) the Gulf of Aqaba system, trending NNE. Many east-trending faults are also present.

The analytical signal (AS) map (Fig. 6) shows strips or ribbons of the most prominent NW-striking magnetic anomaly trends that can be correlated with dikes intruded through pre-existing faults as indicated by dashed white lines in Fig. 6. It is clear from the AS map (Fig. 6) that numerous dikes intruded the Midyan East terrane where the Ifal and Muwaylih Suites compared with relatively few dikes that intruded the Midyan and Haql granites, indicated by white ellipses in Fig. 6. This indicates that the density of dikes is dependent on the availability of fractures in the rocks they intrude (Fig. 7). No dikes intruded the Paleozoic rocks of Hadabet Hisma in the northeastern part of the study area, possibly because of its position out of the influence of the Red Sea rifting.

5 EARTHQUAKE DISTRIBUTION AND SEISMOTECTONICS

Earthquakes that affect northwestern Arabian Plate have been collected from local and regional data sources including historical (112–1964 AD) and instrumental (1964–2010) earthquakes. The compiled catalogue has been correlated with the regional catalogues of Poirier and Taher (1980); Ambraseys et al. (1994) and Abou Elenean (1997) and also has been checked with the on-line bulletin international earthquake data centers of the International Seismological Center (ISC) and European Mediterranean Seismological Center (EMSC). The different types of magnitude given in these sources were converted into a unified body-wave magnitude (*M*b) following Ambraseys and Free (1997), Al-Amri (1995) and Ambraseys and Bommer (1990). Finally, the earthquake catalogue results (Table 1) are presented as an overlay on the interpreted structure map to construct a seismotectonic map of the Midyan area (Fig. 8).

The majority of recorded earthquakes are concentrated in the Gulf of Aqaba, where their moment magnitude (*M*w) ranges from 3.0 up to 7.3, although earthquakes have occurred

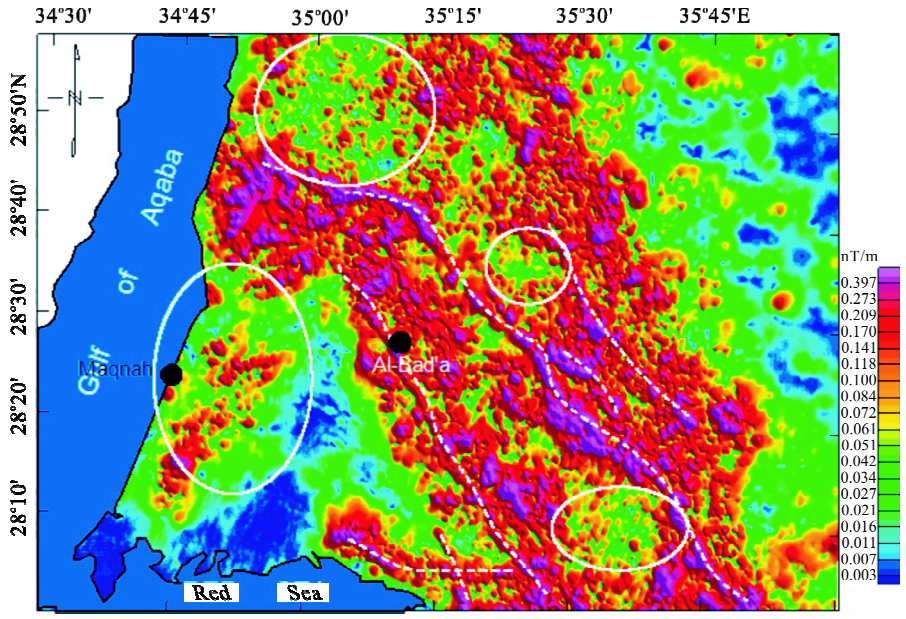

Figure 6. Analytic signal (AS) map of the study area showing localities intruded by basic dikes. For dashed lines and ellipses, see text.

Figure 7. Basic dike intruding a structural weakness zone in the Muwaylih Suite.

inland near the Gulf of Aqaba as well. The Gulf of Aqaba is considered as a continuation of the active Levant fault (Kebeasy, 1990). Instrumentally recorded earthquake activity continued from January to April 1983 when more than 500 earthquakes reaching a magnitude of 4.8 were recorded in the Gulf of Aqaba and caused widespread concern (Shapira and Jarradat, 1995; El-Isa et al., 1984). An earthquake swarm from August 1993 to February 1994 reached magnitudes up to 5.8, to the south of the 1983 swarm. On 22nd November, 1995, the largest earthquake in the Gulf of Aqaba (Mw=7.3) struck the area followed by more than 1 000 aftershocks where the length of the after-shocks area reach about 110 km.

The epicentral distribution of earthquakes shows that the epicenters are oriented mainly NNE parallel to the strike of the Gulf of Aqaba although there are some earthquakes aligned

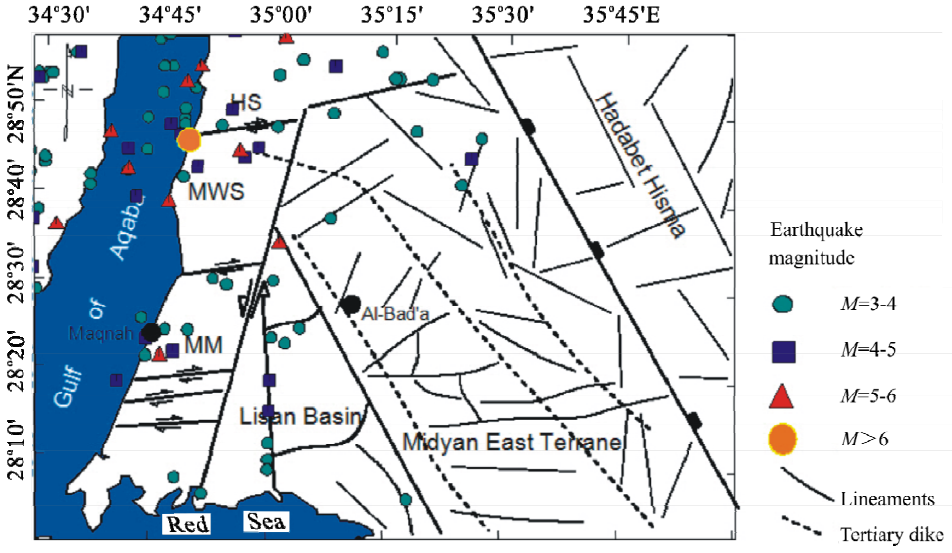

Figure 8. Seismotectonic map of the Midyan area.

Table 1 List of selected earthquakes and their source parameters

No.	D	M	Year	Origin time			Lat	Long	Mag.	No.	D	M	Year	Origin time			Lat	Long	Mag.
				H	Min	Sec	(°N)	(°E)	(*M*b)					H	Min	Sec	(°N)	(°E)	(*M*b)
1	10	5	1969	9	27	0	27.5	34.2	4.8	18	2	6	1996	17	33	13.3	27.66	34.28	3.5
2	28	6	1972	9	49	35	27.7	33.8	5.5	19	9	6	2004	11	41	16.03	27.84	36.97	3.9
3	23	3	1982	10	48	31	27.9	34.29	4.7	20	22	6	2004	14	38	58.65	27.81	36.97	5.1
4	30	10	1982	4	36	46.2	27.8	34	4.5	21	3	8	1993	16	33	21	28.79	34.59	5.4
5	31	12	1985	19	42	0	28.95	35.05	5.3	22	4	11	1994	6	0	48	27.43	34.45	3.2
6	9	9	1989	5	16	0	28.57	34.82	4.1	23	1	12	2002	12	13	23.8	27.29	34.74	3.6
7	3	8	1993	12	43	5	28.78	34.57	5.9	24	25	6	2000	19	18	48	28.21	33.48	4.6
8	3	8	1993	16	33	23.6	28.36	34.08	5.7	25	7	12	2002	12	13	23.8	27.29	34.74	3.6
9	15	4	1995	22	5	5.9	27.608	33.836	3.2	26	16	3	1996	16	3	17.29	29	34.4	3.9
10	12	5	1995	18	11	38.5	27.669	33.764	3.2	27	31	3	1969	7	15	54	27.61	33.91	6.1
11	22	11	1995	4	15	11	28.83	34.79	6.2	28	20	8	2001	15	55	10	27.49	33.92	3.1
12	22	11	1995	22	16	53	28.52	34.7	5	29	25	10	2002	18	4	41.6	27.53	33.62	3.8
13	23	11	1995	18	7	17	29.33	34.74	5.2	30	22	11	1995	12	47	0	28.55	34.72	5.2
14	31	12	1995	6	48	14.3	27.513	34.017	3.3	31	3	11	1993	18	39	32	28.7	34.65	4.8
15	21	2	1996	4	59	51	28.8	34.78	5.3	32	8	11	1993	1	6	2	28.69	34.65	4.8
16	24	4	1996	21	59	32.9	27.656	34.28	3.5	33	4	12	1993	23	34	11	28.88	34.9	4.9
17	25	4	1996	21	59	1.2	27.653	34.3	3.5	34	30	7	1993	23	34	10	28.86	34.82	4.7

D. Day; M. month; H. hour; Min. minute; Sec. second; Lat. latitude; Long. longitude; Mag.. megnatism.

along a nearly N-S fault in the southwestern zone of the study area close to the northern edge of the Red Sea that may reflect a northern extension of active Red Sea tectonics (Fig. 8). The western part of the study area (domain C) exhibits a number of earthquakes closely located along the ENE fault structures. There are a number of earthquakes around Maqnah extending close to ENE inland with magnitudes ranging from 3.0 up to 6.0. The dense distribution of earthquakes in the southern Gulf of Suez-northern Red Sea zone is attributed to predominant tensile stresses in the gulf (Shwartz and Arden, 1960). The greatest earthquake in this area (*M*b 6.9) occurred on March 31, 1969 under Shadwan Island (Fairhead and Girdler, 1971). The epicenteral distribution at the southern Gulf of Suez extends toward the active median zone of the northern Red Sea rift.

The fault plane solutions of the earthquakes (Table 2 and Fig. 9) make it clear that two types of faulting affected the study area; normal faulting (e.g., the Tabuk earthquakes) and strike-slip faulting (e.g., along the Gulf of Aqaba). This reflects, to a great extent, two major tectonic trends prevailing in the area: (1) the Gulf of Aqaba trend and (2) the Red Sea trend. The focal mechanism of the Aqaba Earthquake 1995 and some aftershocks presents a strike-slip movement with predominant normal components except for one event on the eastern side of the Gulf of Aqaba that shows strike-slip with a reverse compo-

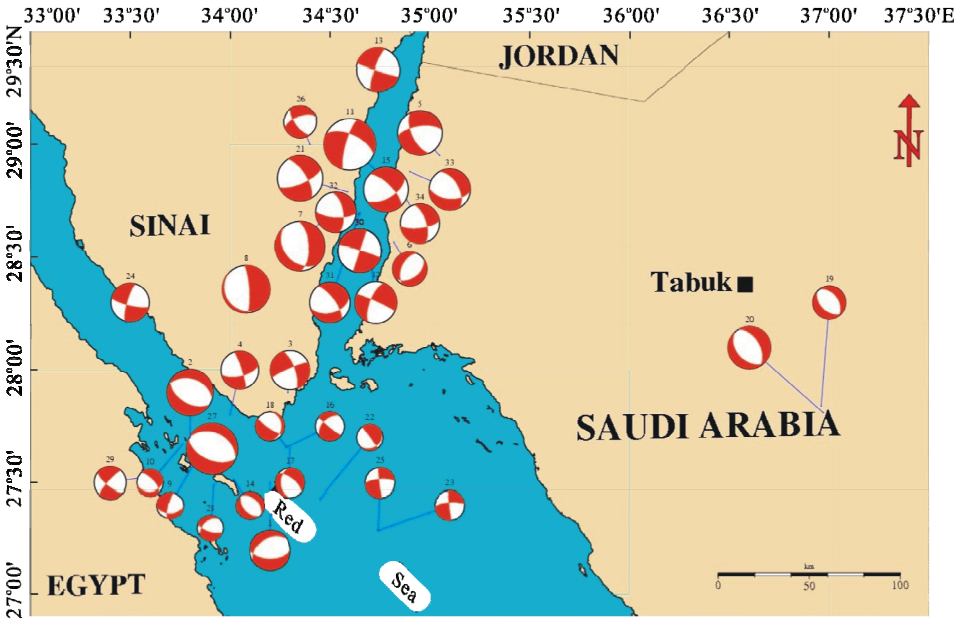

Figure 9. Fault plane solutions for some earthquakes in the study area.

Table 2 Focal mechanisms of selected earthquakes

No.	D	M	Year	Lat (ºN)	Long (ºE)	Plane -1		Plane -2		Reference
						Strike1	Dip1	Strike2	Dip2	
1	10	5	1969	27.5	34.2	237	39	90	55	Salamon et al. (2003)
2	28	6	1972	27.7	33.8	288	40	121	51	Huang and Solomon (1987)
3	23	3	1982	27.9	34.29	247	82	340	76	Mousa (1989)
4	30	10	1982	27.8	34.00	342	82	76	72	Mousa (1989)
5	31	12	1985	28.95	35.05	261	64	155	60	Salamon et al. (2003)
6	9	9	1989	28.57	34.82	205	50	54	43	Salamon et al. (2003)
7	3	8	1993	28.78	34.57	139	36	357	60	HRV (CMT)
8	3	8	1993	28.36	34.05	142	13	356	79	HRV (CMT)
9	15	4	1995	27.61	33.83	196	75	89	45	HRV (CMT)
10	12	5	1995	27.66	33.76	82	35	316	68	HRV (CMT)
11	22	11	1995	28.83	34.79	294	59	196	77	PDE
12	22	11	1995	28.52	34.7	202	67	294	87	PDE
13	23	11	1995	29.33	34.74	199	77	108	83	PDE
14	31	12	1995	27.51	34.01	313	42	136	48	Hussein et al. (2006)
15	21	2	1996	28.8	34.78	315	69	59	60	Abou Elenean (1997)
16	24	4	1996	27.65	34.28	225	47	129	84	Hussein et al. (2006)
17	25	4	1996	27.65	34.3	181	37	308	66	Hussein et al. (2006)
18	2	6	1996	27.66	34.28	124	77	1	22	Hussein et al. (2006)
19	9	6	2004	27.84	36.97	324	44	133	47	Al-Damegh et al. (2009)
20	22	6	2004	27.81	36.97	137	40	329	50	Al-Damegh et al. (2009)
21	3	8	1993	28.79	34.59	328	67	67	70	HRV (CMT)
22	4	11	1994	27.43	34.45	323	88	58	30	Abou Elenean (1997)
23	1	12	2002	27.29	34.74	174	87	265	75	ENSN (2002)
24	25	6	2000	28.21	33.48	196	77	103	76	ENSN (2000)
25	7	12	2002	27.29	34.74	174	87	265	75	ENSN (2002)
26	16	3	1996	29.00	34.40	145	65	249	63	HRV (CMT)
27	31	3	1969	27.61	33.91	294	37	113	53	Huang and Solomon (1987)
28	20	8	2001	27.49	33.92	229	40	108	67	ENSN (2001)
29	25	10	2002	27.53	33.62	222	79	128	67	ENSN (2002)
30	22	11	1995	28.55	34.72	288	88	18	78	Salamon et al. (2003)
31	3	11	1993	28.7	34.65	324	69	75	47	Abou Elenean (1997)
32	8	11	1993	28.69	34.65	350	60	93	69	Abou Elenean (1997)
33	4	12	1993	28.88	34.9	331	54	95	52	Abou Elenean (1997)
34	30	7	1993	28.86	34.82	343	63	83	72	Abou Elenean (1997)

HRV (CMT). Harvard University Centroid Moment Tensor; PDE. preliminary determination of epicenters; ENSN. egyptian national seismological network. D. Day; M. month; Lat. latitude; Long. longitude.

nent in NNW and ENE trending planes (Korrat et al., 2006; Abou Elenean, 1997). The centroid moment tensor computed by Harvard University for the two largest earthquakes of magnitudes 5.8 and 5.6 respectively shows a north-south striking fault with a reverse component.

6 DISCUSSION AND CONCLUSIONS

Interpretation of the aeromagnetic data shows that the causative bodies of magnetic anomalies are characteristic and have distinctive signatures. Low magnetic anomalies dominate the eastern and southwestern sides of the study area; relatively high magnetic anomalies dominate the western side, while the middle part is characterized by rapid local variations in magnetic intensity and anomaly pattern. Based on the trends, patterns and intensity of the magnetic anomalies, the study area is divided into four major domains by two fault systems extending in NNE and NNW directions. Left-lateral strike-slip displacement of ENE faults by the NNE trend predominates in the western side along the Gulf of Aqaba coast and stops at the boundary of the Midyan East terrane. It is interesting to observe from the earthquake distribution map for the period 1969–2004 that a seismic quiescent region coincides with the absence of these strike-slip movements in the previously defined Midyan East terrane. In the Midyan East terrane the causative bodies of NNW extending magnetic anomalies correlate with dikes that filled pre-existing NNW-oriented faults. The northern terminations of the NNW-oriented dikes become WNW-oriented, indicating the northern termination of the Red Sea rift and transfer of movement to WNW-oriented faults. The occurrence of the NNW-oriented dikes is restricted to the Midyan East terrane, indicating deep-seated faults through which the magma ascended.

The structural trends deduced from the aeromagnetic maps are confirmed by seismological fault plane solution re-

sults. The hypocentral distribution of earthquakes illustrates the prevalence of the NW-SE, ENE and NNE-SSW faulting trends. The fault plane solutions for the largest earthquakes in the study area indicate that there are mixed mechanisms between extensional and strike-slip faulting. The Gulf of Aqaba is characterized mainly by strike-slip faulting mechanisms while the neighboring Tabuk zone is of normal dip-slip faulting. Accordingly, the study area displays different mechanisms associated with different tectonic trends which are indicated clearly in the structural pattern controlling the area. At the northwestern part of the study area the wrench tectonics of the Gulf of Aqaba intersect pre-existing structural elements.

ACKNOWLEDGMENT

The authors would like to extend their sincere appreciation to the Deanship of Scientific Research at King Saud University for funding this research group (No. RG-1436-011). The final publication is available at Springer via http://dx.doi.org/10.1007/S12583-016-0904-0.

REFERENCES CITED

Abou Elenean, K., 1997. A Study on the Seismotectonics of Egypt in Relation to the Mediterranean and Red Sea Tectonics: [Dissertation]. Ain Shams University, Cairo. 156

Afifi, A. M., Connally, T. C., Senalp, M., et al., 1993. Preliminary Report on a Geologic Field Trip to Midyan, December 11–19, 1992. Saudi Aramco Geological Research and Development Division, Miscellaneous Report 995. 14

Al-Amri, A. M., 1995. Recent Seismic Activity in the Northern Red Sea. *Journal of Geodynamics*, 20(3): 243–253. doi:10.1016/0264-3707(95)00007-V

Al-Damegh, K. S., Abou Elenean, K. M., Hussein, H. M., et al., 2009. Source Mechanisms of the June 2004 Tabuk Earthquake Sequence, Eastern Red Sea Margin. *Kingdom of Saudi Arabian Journal Seismology*, 13(4): 561–576. doi: 10.1007/s10950-008-9148-5

Al-Fotawi, B. A., Gazzaz, M. A., Hassan, M. A., 1991. Uranium and Thorium Enrichment in Haql Granite in Midyan Region, Northwest of Saudi Arabia. *Earth Sciences Journal*, 4(1): 161–170. doi:10.4197/ear.4-1.9

Al-Rehaili, M. H., 1982. Reconnaissance Geology of the Wadi as Sahab Quadrangle, Sheet 28/35B. Kingdom of Saudi Arabia, Saudi Arabian Deputy Ministry for Mineral Resources, Jeddah. Open-File Report DGMR-OF-02-12. 14

Ambraseys, N. N., Bommer, J. J., 1990. Uniform Magnitude Re-Evaluation for the Strong-Motion Database of Europe and Adjacent Areas. *Journal of European Earthquake Engineering*, 4: 3–16

Ambraseys, N. N., Free, M. W., 1997. Surface-Wave Magnitude Calibration for European Region Earthquakes. *Journal of Earthquake Engineering*, 1(1): 1–22. doi:10.1080/13632469708962359

Ambraseys, N. N., Melville, C. P., Adams, R. D., 1994. The Seismicity of Egypt, Arabia and the Red Sea. In: Ambraseys, N. N., Melville, C. P., Adams, R. D., eds., Cambridge University Press, Cambridge. 181

Andreasen, G. E., Petty, A. J., 1974. Total Intensity Aeromagnetic Map of the Northern Hijaz Quadrangle and Part of Wadi as Sirhan Quadrangle, Kingdom of Saudi Arabia. Directorate General of Mineral Resources, Saudi Arabian. Geologic Map GM-9, Scale 1 : 500 000

Bird, D., 1997. Interpreting Magnetic Data: Geophysical Corner. AAPG Explorer, May, 1997, Houston

Blank, H. R., 1977. Aeromagnetic and Geologic Study of Tertiary Dikes and Related Structures on the Arabian Margin of the Red Sea. In: Hilpert, L. S., ed., Red Sea Research 1970–1975. *Saudi Arabian Directorate General of Min. Res.*, 22: G1–G18

Bramkamp, R. A., Brown, G. F., Holme, D. A., et al., 1963. Geologic Map of the Wadi as Sirhan Quadrangle, Kingdom of Saudi Arabia, Jeddah. U.S. Geological Survey Miscellaneous Geological Investigations Map I-200 A, Scale 1 : 500 000

Clark, M. D., 1985. Geologic Map of the Al Bad' Quadrangle, Sheet 28A, Kingdom of Saudi Arabia. Saudi Arabian Directorate General of Mineral Resources, Jeddah. Geoscience Map GM-81, Scale 1 : 250 000. 46

Clark, M. D., 1987. Geologic Map of the Al Bad' Quadrangle, Sheet 28A, Kingdom of Saudi Arabia. Ministry of Petroleum and Mineral Resources, Deputy Ministry for Mineral Resources, Jeddah. Geoscience Map GM-81, Scale 1 : 250 000

Davies, F. B., Grainger, D. J., 1985. Geologic Map of the Al Muwaylih Quadrangle, Sheet 27A. Kingdom of Saudi Arabia: Saudi Arabian Deputy Ministry for Mineral Resources, Jeddah. Geoscience Map GM-82, Scale 1 : 250 000. 32

El-Isa, Z., Merghelani, H., Bazzaris, M., 1984. The Gulf of Aqaba Earthquake Swarm of 1983 January–April. *Geophysics Journal of Royal Astronomical Society*, 78(3): 711–722. doi: 10.1111/j.1365-246.1984.tb05066.x

Fairhead, J. D., Girdler, R. W., 1971. The Seismicity of Africa. *Geophysical Journal International*, 24(3): 271–301. doi:10.1111/j.1365-246x.1971.tb02178.x

Harris, N. B. W., 1985. Alkaline Complexes from the Arabian Shield. *Journal of African Earth Sciences*, 3(1–2): 83–88. doi:10.1016/0899-5362(85)90025-9

Huang, P. Y., Soloman, S. C., 1987. Centroid Depth and Mechanisms of Mid-Ocean Ridge Earthquakes in the Indian Ocean. Gulf of Aden, and Red Sea. *Journal of Geophysical Research*, 92: 1361–1382

Hughes, G. W., Perincek, D., Grainger, D. J., et al., 1999. Lithostratigraphy and Depositional History of Part of the Midyan Region, Northwestern Saudi Arabia. *GeoArabia*, 4(4): 503–542

Hussein, H. M., Marzouk, I., Moustafa, A. R., et al., 2006. Preliminary Seismicity and Focal Mechanisms in the Southern Gulf of Suez: August 1994 through December 1997. *Journal of African Earth Sciences*, 45(1): 48–60. doi:10.1016/j.jafrearsci.2006.01.006

Ibrahim, E. H., Odah, H. H., El Agami, N. L., et al., 2000. Paleomagnetic and Geological Investigation into Southern Sinai Volcanic Rocks and the Rifting of the Gulf of Suez. *Tectonophysics*, 321(3): 343–358. doi:10.1016/s0040-1951(00)00066-4

Johnson, R. F., Trent, V. A., 1967. Mineral Reconnaissance of

Wadi as Surr Quadrangle, Kingdom of Saudi Arabia. Saudi Arabian Directorate General of Mineral Resources, Jeddah. Mineral Investigation Map MI-5, Scale 1 : 100 000

Kebeasy, R. M., 1990. Seismicity in Geology of Egypt. In: Rushdi Said, ed., The Geology of Egypt. A A Balkerma, Rotterdam. 51–59

King Fahd University of Petroleum and Minerals (KFUPM), 1998. Processing and Interpretation of Landsat TM Data for the Midyan Area, Red Sea. Unpublished Report for Saudi Aramco, Dhahran. 49

Korrat, I., Hussein, H., Marzouk, I., et al., 2006. Seismicity of the Northernmost Part of the Red Sea (1995–1999). *Acta Geophysica*, 54(1): 33–49. doi:10.2478/s11600-006-0004-0

Milner, A., Morris, N., Jeffery, P., 1993. Report on Macrofossils from the Kingdom of Saudi Arabia. Natural History Museum, London

Motti, E., Teixido, L., Vazques-Lopez, R., et al., 1982. Maqna Massif Area: Geology and Mineralization. Saudi Arabian Deputy Ministry for Mineral Resources Open File Report BRGM-OF-02-16. 44

Mousa, H. M., 1989. Earthquake Activities in Egypt and Adjacent Regions and Its Relation to Geotectonic Features in A. R. Egypt: [Dissertation]. Mansoura University, Mansoura

Moustafa, A. R., Abd-Allah, A. M., 1992. Transfer Zones with En Echelon Faulting at the Northern End of the Suez Rift. *Tectonics*, 11(3): 499–506. doi:10.1029/91tc03184

Poirier, J. P., Taher, M. A., 1980. Historical Seismicity in the Near and Middle East, North Africa, and Spain from Arabic Documents (VIIth-XVIIIth Century). *Bulletin of the Seismological Society of America*, 70: 2185–2201

Radain, A. A. M., 1980. Petrogenesis of Some Peralkaline and Non-Peralkaline Post-Tectonic Granites in the Arabian Shield, Kingdom of Saudi Arabia. *Faculty of Earth Sciences*, *KAU Jeddah*, *Research*, 16: 195

Ramsay, C. R., Drysdall, A. R., Clark, M. D., 1986. Felsic Plutonic Rocks of the Midyan Region, Kingdom of Saudi Arabia—I, Distribution, Classification, and Resource Potential. In: Drysdall, A. R., Ramsay, C. R., Stoeser, D. B., eds., Felsic Plutonic Rocks and Associated Mineralization of the Kingdom of Saudi Arabia. *Saudi Arabian Deputy Ministry for Mineral Resources Bulletin*, 29: 63–77

Remond, C., Teixido, L., 1980. Geological and Mineral Exploration of the Sedimentary Cover between Al Bad and Al Muwaylih (28/35 A-C and 27/35 A-B). Bureau de Recherches Géologiques et Minères Open-File Report JED-OR 80–26. 79

Rowaihy, N. M., 1985. Geologic Map of the Haql Quadrangle, Sheet 29A, Kingdom of Saudi Arabia. Saudi Arabian Directorate General of Mineral Resources, Jeddah. Geoscience Map GM-80, Scale 1 : 250 000. 15

Salamon, A., Hofstetter, A., Garfunkel, Z., et al., 2003. Seismotectonics of the Sinai Subplate—The Eastern Mediterranean Region. *Geophysical Journal International*, 155(1): 149–173. doi:10.1046/j.1365-246x.2003.02017.x

Shapira, A., Jarradat, M., 1995. Earthquake Risk and Loss Assessment in Aqaba and Eilat Regions. The U.S. Aid-Merc Program. The Institute for Petroleum Research and Geophysics, Israel

Shwartz, D. H., Arden, D. D., 1960. Geological History of the Red Sea Area. *American Association of Petroleum Geologists Bulletin*, 44: 1621–1637

Stoeser, D. B., 1986. Distribution and Tectonic Setting of Plutonic Rocks of the Arabian Shield. *Journal of African Earth Sciences*, 4: 21–46. doi:10.1016/s0899-5362(86)80066-5